

THE APPLICATION OF MODULATED DIFFERENTIAL SCANNING CALORIMETRY TO THE GLASS TRANSITION

Theoretical analysis using a single parameter model

*J. M. Hutchinson*¹ and *S. Montserrat*²

¹Engineering Department, Aberdeen University, Aberdeen AB9 2UE, Scotland, UK

²Laboratori de Termodinàmica ETSEIT, Departament de Màquines i Motors Tèrmics, Universitat Politècnica de Catalunya, Carrer de Colom 11, 08222 Terrassa, Barcelona, Spain

Abstract

The modulated differential scanning calorimetry (MDSC) technique superimposes upon the conventional DSC heating rate a sinusoidally varying modulation. The result of this modulation of the heating rate is a periodically varying heat flow, which can be analysed in various ways. In particular, MDSC yields two components ('reversing' and 'non reversing') of the heat flow, and a phase angle. These each show a characteristic behaviour in the glass transition region, but their interpretation has hitherto been unclear. The present work clarifies this situation by a theoretical analysis of the technique of MDSC, which introduces a kinetic response of the glass in the transition region. This analysis is able to describe all the usual features observed by MDSC in the glass transition region. In addition, the model is also able to predict the effects of the modulation variables, and some of these are discussed briefly.

Keywords: glass transition, MDSC

Introduction

The technique of modulating conventional differential scanning calorimetry appears to be growing in popularity since the introduction a few years ago by Reading [1-4]. The original concept was commercialised by TA Instruments as Modulated Differential Scanning Calorimetry (MDSC), but other variants are also available, e.g. Oscillating (ODSC, from Seiko Instruments), Dynamic (DDSC, from Perkin Elmer) and Alternating (ADSC, from Mettler Toledo) systems. The basic principle is to superimpose upon the conventional DSC heating rate a periodically varying temperature modulation. In MDSC, this modulation is sinusoidal, giving a time (t) dependent temperature (T) as:

* Author to whom all correspondence should be addressed.

$$T = T_0 + q_{av}t + A_T \sin(\omega t) \quad (1)$$

where T_0 is the initial temperature for the MDSC scan, q_{av} is the average or underlying heating rate, A_T is the amplitude of the temperature modulation, and ω is the angular frequency of modulation.

Analysis of MDSC has hitherto been rather limited, the most complete works [5, 6] being based upon the thermal lag between sample and programme temperatures. No analysis, however, has yet been able to describe the interesting features of the data which emerge from the deconvoluted MDSC signal in the glass transition region. The result of the modulation of the heating rate is a periodically varying heat flow, which can be analysed in various ways. In particular, the method adopted by Reading [1-4] and used by TA Instruments introduces the following features: (i) a 'step change' in the so-called 'reversing' heat flow; (ii) the appearance of a peak in the so-called 'non-reversing' heat flow; and (iii) a phase angle between heating rate and heat flow, which passes through a maximum in the transition region. Another method of evaluation of MDSC response is based on linear response theory [6] and yields a complex heat capacity with a real part or storage heat capacity, and an imaginary part or loss heat capacity.

Here, we present a theoretical analysis in which a fundamentally different approach is taken. The analysis assumes infinitely good heat transfer between instrument and sample, but introduces a kinetic response for the relaxation occurring in the glass transition region. The paper clarifies the interpretation of the results obtained by the MDSC technique, and analyses the effect of modulation variables on the heat flow response.

Theory

Previous theoretical analyses of MDSC have been rather limited [4-7] and have been based upon the kinetics of heat transfer between instrument and sample. In other words, no analysis has yet considered the kinetics of relaxation effects within the sample itself at the glass transition. In order to include these effects, the starting point here is the differential equation used previously [8] to describe the kinetics of enthalpy (H) relaxation during conventional DSC runs:

$$\frac{d\delta}{dt} = -\Delta C_p q - \frac{\delta}{\tau(T, \delta)} \quad (2)$$

In this equation, $\delta = H - H_\infty$ is the excess enthalpy relative to the equilibrium value (H_∞), ΔC_p is the difference between the liquid (C_{pl}) and glassy (C_{pg}) specific heat capacities, and q is the heating rate, given by the time derivative of Eq. (1):

$$q = q_{av} + A_T \omega \cos(\omega t) \quad (3)$$

Figure 1 shows the modulation of the temperature and of the heating rate for an underlying heating rate of 2.5 K min^{-1} , a period of 24 s, and a temperature amplitude (A_T) of 0.25 K. The corresponding amplitude of the heating rate ($A_q = A_T \omega$) is 3.93 K min^{-1} . These experimental conditions are typical of those used in MDSC, and have been used often in the work presented here.

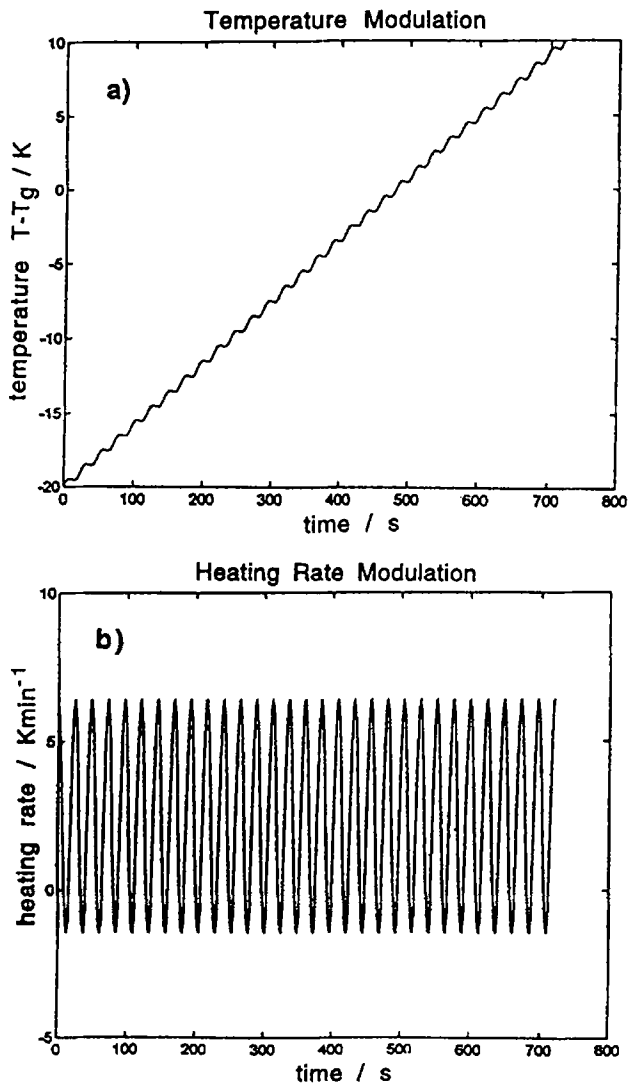


Fig. 1 Temperature modulation (a), and heating rate modulation (b) for an average heating rate of 2.5 K min^{-1} , a period of 24 s, and a temperature amplitude of 0.25 K

The single relaxation time τ depends [8] upon both T and δ , according to:

$$\tau = \tau_g \exp[-\theta(T - T_g)] \exp\left[-\frac{(1-x)\theta\delta}{\Delta C_p}\right] \quad (4)$$

where τ_g is the relaxation time in equilibrium at the glass transition temperature T_g , x is the non-linearity parameter ($0 \leq x \leq 1$), and θ is a constant defining the temperature dependence of τ , given by the approximation:

$$\theta \approx \frac{\Delta h^*}{RT_g^2} \quad (5)$$

where Δh^* is an apparent activation energy.

Equations (2) and (4) define the response of the glass to any prescribed thermal history, and in particular to that defined by Eq. (1). This system of equations has been solved numerically for several combinations of experimental variables [q_{nv} , period ($2\pi/\omega$), A_T and initial state (δ_0) at T_0] in order to obtain the variation of the excess enthalpy δ with time (or temperature). The heat flow HF is then determined by the following equations derived from Eq. (2) and the definition of δ :

$$HF = \frac{dH}{dt} = C_{p,l} q + \frac{d\delta}{dt} = C_{p,g} q - \frac{\delta}{\tau(T, \delta)} \quad (6)$$

Results and discussion

A. Solution of the single parameter model

The differential Eq. (2) was solved by a numerical integration using a 4th–5th order Runge-Kutta routine, with the following material constants: $C_{pl} = 1.6 \text{ J g}^{-1} \text{ K}^{-1}$; $C_{pg} = 1.3 \text{ J g}^{-1} \text{ K}^{-1}$, $\Delta C_p = 0.3 \text{ J g}^{-1} \text{ K}^{-1}$, $\tau_g = 100 \text{ s}$, $\theta = 1.0 \text{ K}^{-1}$ [$\Delta h^* = 1200 \text{ kJ mol}^{-1}$ for $T_g \approx 105^\circ\text{C}$], $x = 0.4$, $\delta_0 = 6 \text{ J g}^{-1}$ ($q_1 \approx -20 \text{ K min}^{-1}$, no annealing) and the temperature range was from $T_g - 20 \text{ K}$ to $T_g + 10 \text{ K}$.

Figure 2 shows the response of the excess enthalpy for the experimental conditions given in the caption. It can be seen that the conventional DSC response and that of MDSC are practically identical up to equilibrium at $\delta = 0 \text{ J g}^{-1}$. During the overshoot interval there are differences between the two responses, but when the equilibrium is reached, the two responses again become equal.

A typical response of the heat flow modulation in the glass transition is shown in Fig. 3 for the experimental conditions given in the caption. The glass transition is seen as: (i) a change in average value of heat flow, (ii) a change in amplitude of heat flow, and (iii) a phase difference between the heat flow and

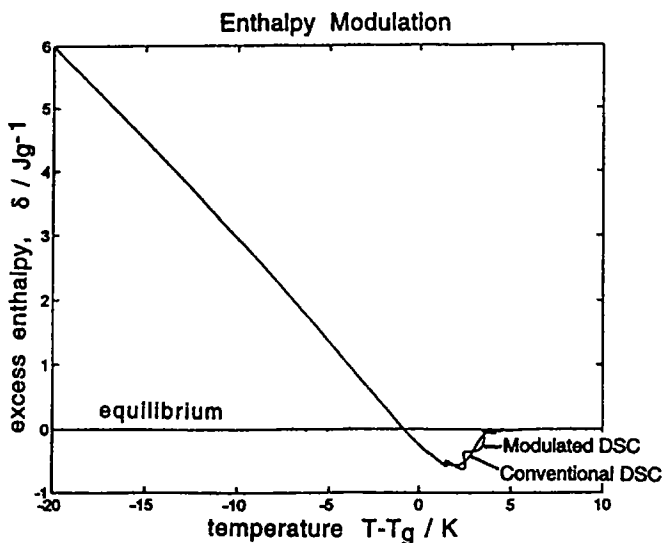


Fig. 2 Enthalpy modulation simulated by the model for the modulation parameters: $q_{av}=2.5 \text{ K min}^{-1}$, period=24 s, and $A_T=0.25 \text{ K}$, with initial condition $\delta_0=6 \text{ J g}^{-1}$. Also shown is the predicted response for conventional DSC at the average heating rate

the heating rate. Figure 3 (c) shows in more detail the phase difference that occurs when the glass becomes a liquid-like system.

The periodically varying heat flow is Fourier transformed cycle-by-cycle and compared with the transform of the cosinusoidally varying heating rate to give dc components $\langle HF \rangle$, the average value of the heat flow, and $\langle q \rangle$, the average value of the heating rate ($=q_{av}$), and first harmonics with amplitudes A_{HF} and A_q for heat flow and heating rate, respectively, and a phase angle φ between heat flow and heating rate. Figure 4 shows these average values and amplitudes in the glassy state for the same experimental conditions as in Fig. 3.

Using Schawe's formulation [6], an average (or total) specific heat capacity, $\langle C_p \rangle$, and complex specific heat capacity, C_p^* , are obtained as:

$$\langle C_p \rangle = \frac{\langle HF \rangle}{\langle q \rangle} \quad (7)$$

$$C_p^* = \frac{A_{HF}}{A_q} \quad (8)$$

The complex heat capacity is out of phase (in general) with the heating rate, and a real part or storage heat capacity, C_p' , and an imaginary part or loss heat capacity, C_p'' , may be assigned [6]:

$$C_p' = C_p^* \cos\phi \quad (9)$$

$$C_p'' = C_p^* \sin\phi \quad (10)$$

These may be compared with the reversing and non-reversing heat flow signals of the TA Instruments MDSC. The reversing heat flow is simply $C_p^* A_q$ (i.e. A_{HF} in Eq. (8)), and is approximately equal to $C_p' A_q$ when the phase angle ϕ is small ($\cos\phi \approx 1$), as is usually the case in the glass transition region. The non-reversing heat flow, which is the difference between the total heat flow and the reversing heat flow, is then given by $\langle C_p \rangle \langle q \rangle - C_p^* A_q$, obtained simply from $\langle HF \rangle - A_{HF}$ in Eqs (7) and (8).

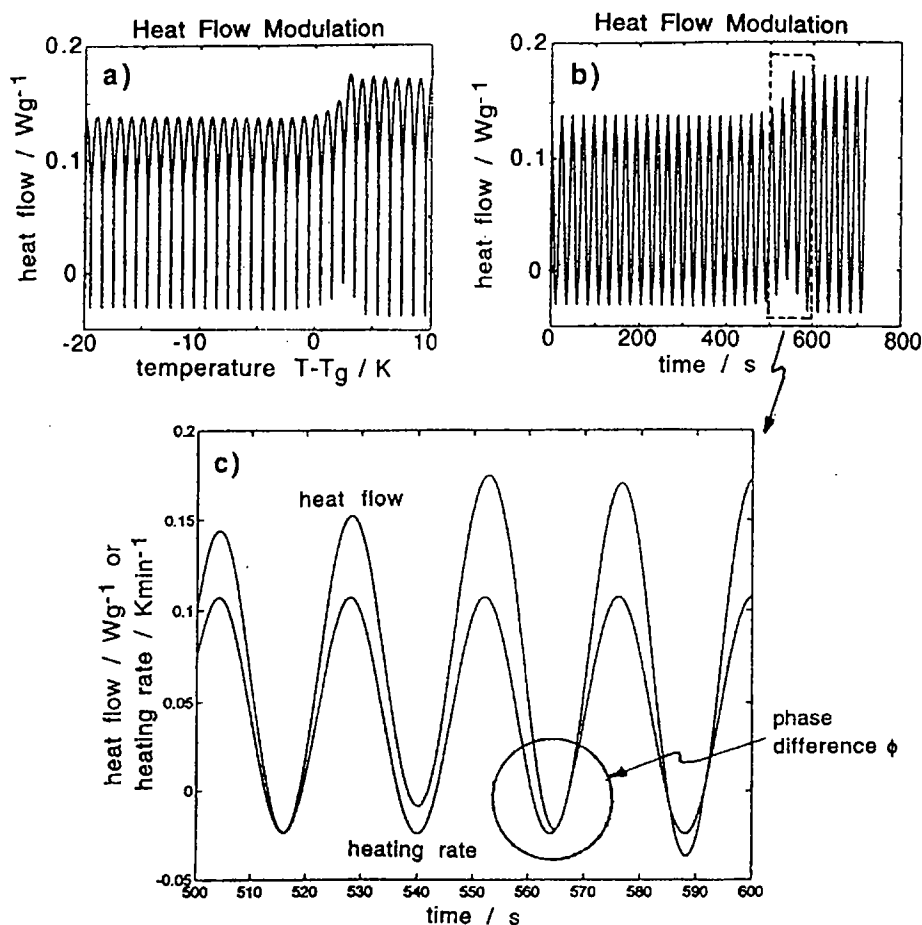


Fig. 3 Heat flow response against temperature (a) and time (b,c) in the glass transition region for the modulation parameters: $q_w = 2.5 \text{ K min}^{-1}$, period = 24 s, and $A_T = 0.25 \text{ K}$

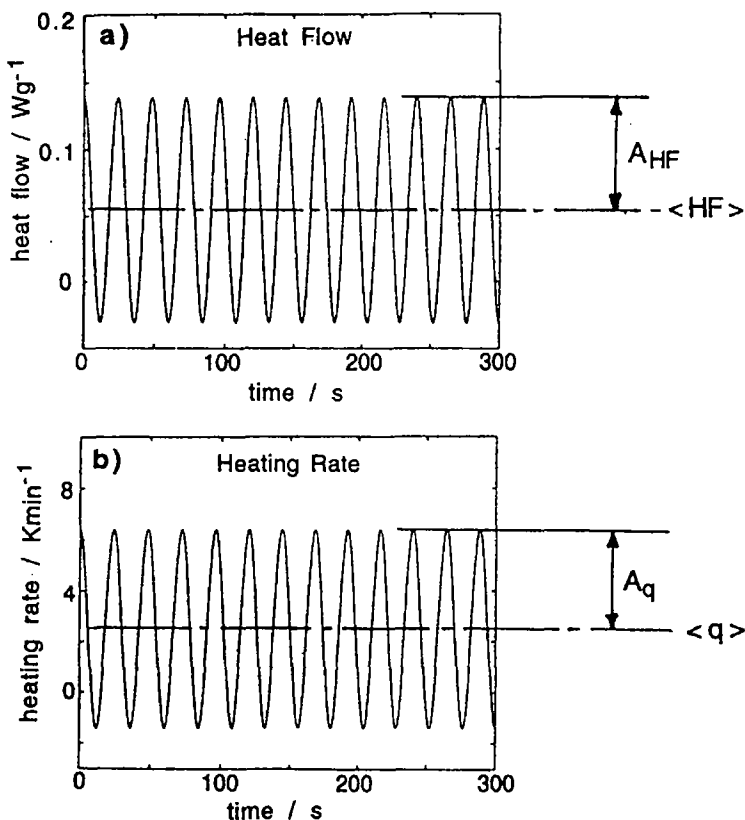


Fig. 4 Average values of the heat flow (a) and the heating rate (b) and their amplitudes in the glassy state for the same experimental conditions as in Fig. 3

The transform of the heat flow shown in Fig. 3 yields the results shown in Fig. 5 for the average heat capacity $\langle C_p \rangle$ (Fig. 5a), storage heat capacity C_p' (Fig. 5b), loss heat capacity C_p'' (Fig. 5c), and phase angle φ (Fig. 5d) during a heating experiment through the glass transition region.

The average heat capacity (Fig. 5a) is very similar to that obtained for conventional DSC with constant heating rate q_{nv} , shown as the full line in Fig. 5a. There are ranges of experimental variables (period, amplitude, q_{nv} , δ_o), though, for which this agreement is predicted by the present model to be much less satisfactory [9].

The storage component C_p' (Fig. 5b) increases from a nearly constant value in the glassy state to a higher value in the liquid-like state, with the transition occurring in general at a different temperature from that of the peak in the average heat capacity (Fig. 5a).

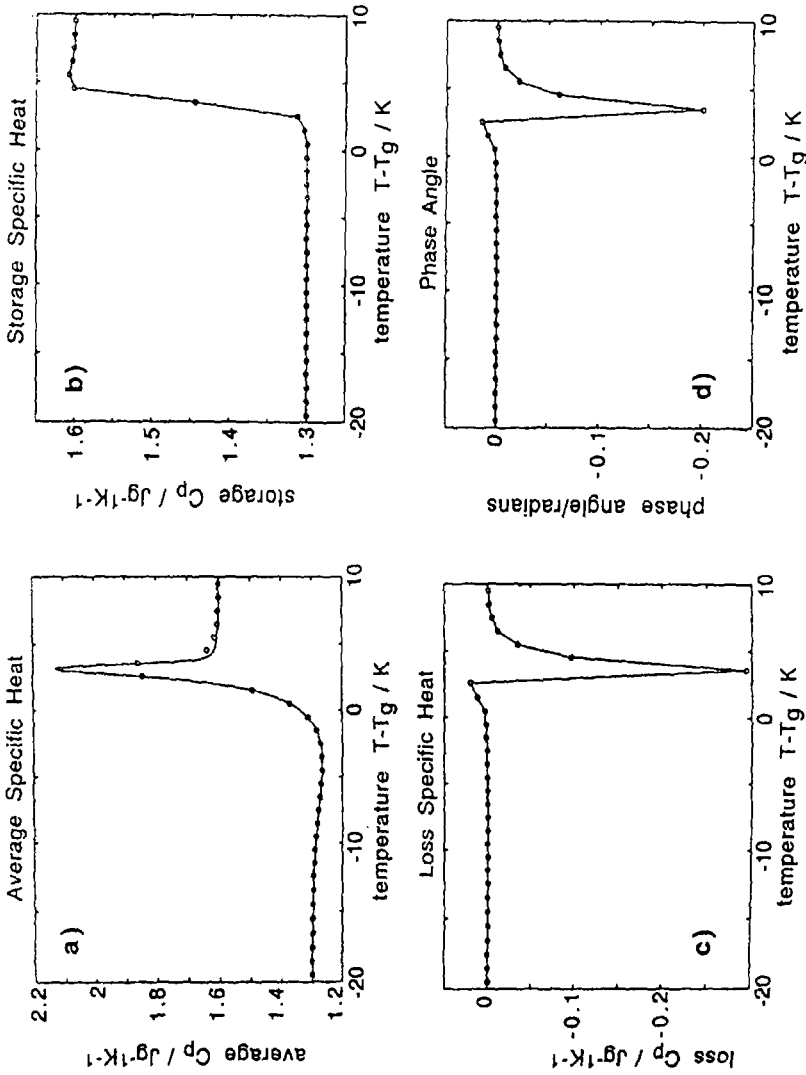


Fig. 5 Specific heat capacities calculated from the heat flow response of Fig. 3 for the same experimental conditions: (a) average heat capacity $\langle C_p \rangle$ for MDSC (points) and for conventional DSC (full line) with a heating rate of 2.5 K min^{-1} ; (b) storage heat capacity, C_p' ; (c) loss heat capacity, C_p'' ; and (d) phase angle, ϕ , vs. temperature. In (b), (c) and (d) the lines are drawn only to join the points, and have no further significance

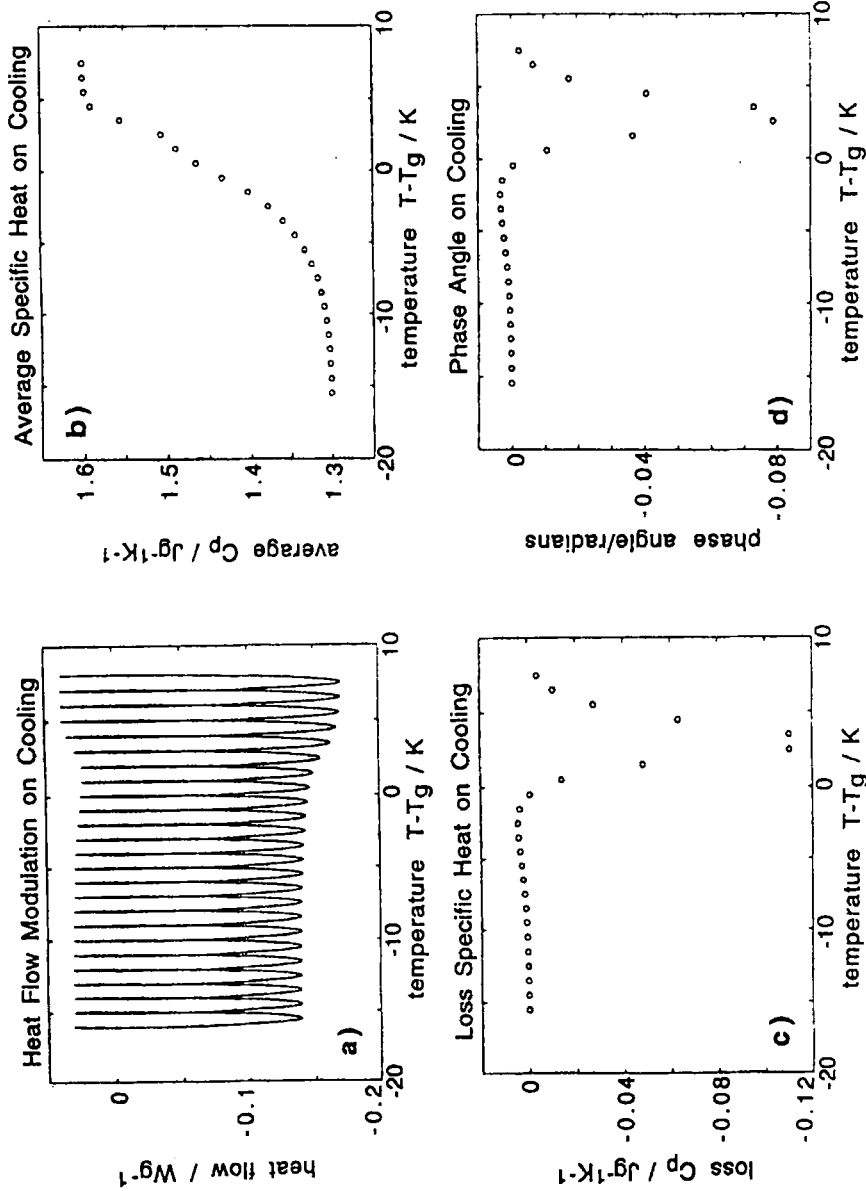


Fig. 6 MDSC cooling experiment: (a) heat flow modulation; (b) average heat capacity; (c) loss heat capacity; (d) phase angle. Experimental conditions: $q_w = -2.5$ K min^{-1} , period = 24 s, and $A_T = 0.25$ K

The phase angle, ϕ (Fig. 5d), departs from zero in the transition from glass to liquid, though the maximum departure is not large (here about 0.2 rads). The negative values indicate that the heat flow lags behind the heating rate in this case. The loss component C_p'' shows a similar dependence to the phase angle (Fig. 5c).

It is interesting also to examine the model prediction for a MDSC trace on cooling. Figure 6a shows the heat flow modulation on cooling, while the average and loss heat capacities, and the phase angle, calculated for the experimental conditions given in the caption, are shown in Figs 6b to 6d.

It should be noted that the peaks in the loss heat capacity and in the phase angle occur in a very similar way both on heating and on cooling. Thus it should not be assumed that the peak in C_p'' results necessarily from an enthalpy relaxation process; it results from the phase angle difference, which itself occurs simply because of the relaxation kinetics in the glass transition region.

B. Effect of modulation variables

Effect of period

The commonly observed [5, 7] change in C_p' (Fig. 5b) from C_{pg} to C_{pl} is explained as follows. At low temperatures the relaxation time is long in

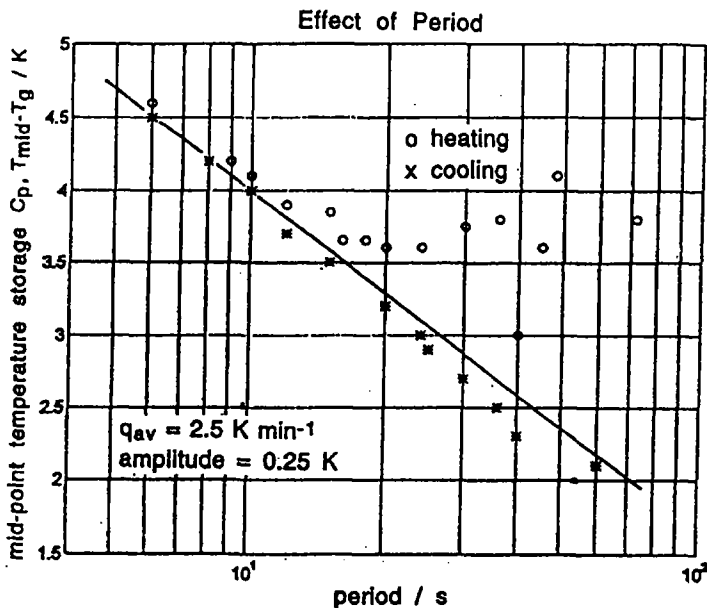


Fig. 7 Mid point temperature for storage heat capacity C_p' vs. period for: an average heating rate of 2.5 K min^{-1} and an amplitude $A_T = 0.25 \text{ K}$ (circles); an average cooling rate of -2.5 K min^{-1} and the same amplitude (crosses). The line is drawn with slope given by $\theta = 1.0 \text{ K}^{-1}$

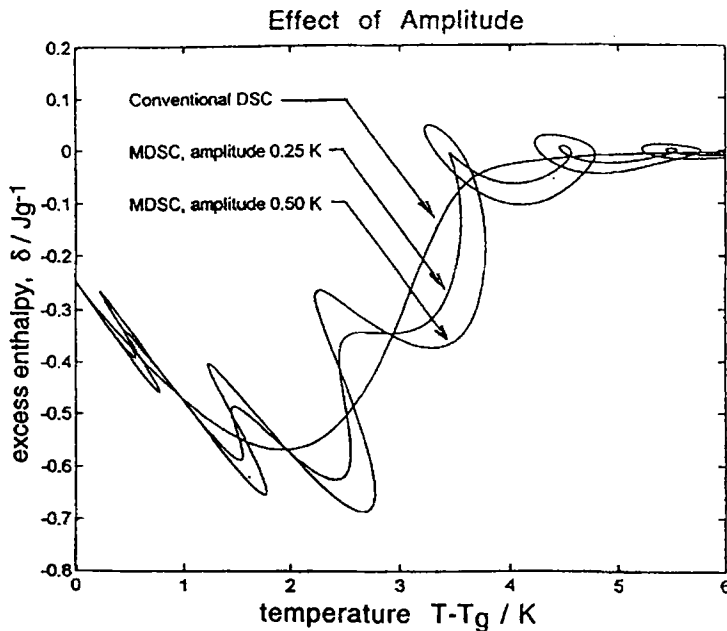


Fig. 8 Effect of amplitude on the excess enthalpy during a heating experiment at average heating rate of 2.5 K min^{-1} , and period of 24 s. Three different simulations are shown: one for conventional DSC, the others for MDSC with amplitudes of temperature modulation 0.25 K and 0.50 K

comparison with the cycle period, and hence the amplitude of the oscillating part reflects a glassy response. On the other hand, at high temperatures the relaxation time is short and the system will follow the equilibrium liquid-like behaviour. The transition occurs when the period approximately equals the relaxation time. Thus the mid-point temperature T_{mid} , at which C_p' passes mid-way between C_{pg} and C_{pl} , will depend upon the period of the cycle. This can be seen in Fig. 7 which shows T_{mid} vs. period in a semilog plot for cycles with an average heating rate of 2.5 K min^{-1} , an amplitude $A_T = 0.25 \text{ K}$, and periods ranging from 6 s to 72 s, as well as for the equivalent MDSC cooling experiment.

Decreasing the period increases the temperature (T_{mid}) at which C_p' passes mid-way between C_{pg} and C_{pl} , and the temperature (T_p) at which C_p'' (and phase angle ϕ) passes through a minimum. Experiments on cooling show a linear dependence of T_{mid} with $\log(\text{period})$ over a wider range than for heating experiments.

Assuming the transition from C_{pg} to C_{pl} occurs approximately when the period equals the relaxation time, and assuming δ is sufficiently small that non-linearity can be ignored, Eq. (4) gives:

$$\frac{d \ln(\text{period})}{dT_{\text{mid}}} = -\theta \quad (11)$$

The line drawn in Fig. 7 has a slope corresponding to the above equation with $\theta = 1.0 \text{ K}^{-1}$ as used in these simulations, and is in good agreement with the results from the transformed heat flow.

Effect of amplitude

Within a reasonable range of amplitude, up to about 0.5 K, the effect of amplitude appears insignificant. With a single relaxation time model, there is no 'memory effect', whereby the response of the glass is a function of the whole of its previous thermal history as a result of a distribution of relaxation times [10, 11]. In the present single relaxation time model, therefore, the response of the glass is a function only of the instantaneous state of the glass, and an increase in the amplitude of temperature modulation leads approximately to a simple scaling in the response of the excess enthalpy δ , as Fig. 8 shows.

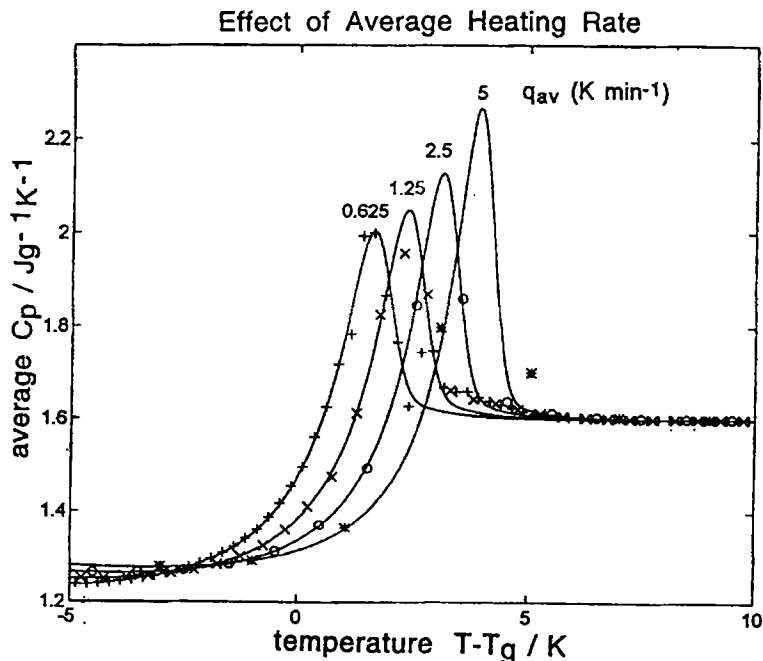


Fig. 9 Effect of average heating rate on the average heat capacity for a period of 24 s, and a temperature amplitude of 0.25 K. The points correspond to the simulated MDSC response and the full lines to the conventional DSC. The heating rates in K min^{-1} are: 0.625 (+); 1.25 (x); 2.5 (o); 5 (*)

Effect of average heating rate

The average heating rate has no effect on C_p' , C_p'' or phase angle, for rates up to about 1.25 K min^{-1} . On the other hand, it does influence the average (or 'total') heat capacity $\langle C_p \rangle$, in approximately the same way as for the conventional DSC, as Fig. 9 shows.

Conclusions

The model for enthalpy relaxation with a single relaxation time describes the commonly observed features of Modulated DSC in the glass transition region. From the theoretical analysis one can derive an average heat capacity $\langle C_p \rangle$ and a complex heat capacity C_p^* . Because the heat flow is out of phase with the heating rate, a phase angle, and hence a storage heat capacity C_p' and a loss heat capacity C_p'' , can be obtained. Results show that the average heat capacity corresponds closely to that for conventional DSC at the same average heating rate.

It has been shown that the transition in C_p' (storage or reversing heat capacity) depends on the period of modulation for both heating and cooling experiments. The phase angle, and hence also C_p'' , departs from and then returns to zero in the transition region. This variation has also been shown to occur in both heating and cooling experiments.

* * *

Financial support has been provided by the DGICYT (Project no.PB93/1241). J.M.H. wishes to acknowledge financial assistance for a sabbatical period from the 'Generalitat de Catalunya'.

References

- 1 J. C. Seferis, I. M. Salin, P. S. Gill and M. Reading, *Proc. Acad. Greece*, 67 (1992) 311.
- 2 P. S. Gill, S. R. Sauerbrunn and M. Reading, *J. Thermal Anal.*, 40 (1993) 931.
- 3 M. Reading, D. Elliott and V. L. Hill, *J. Thermal Anal.*, 40 (1993) 949.
- 4 M. Reading, *Trends Polym. Sci.*, 8 (1993) 248.
- 5 B. Wunderlich, Y. Jin and A. Boller, *Thermochim. Acta*, 238 (1994) 277.
- 6 J. E. K. Schawe, *Thermochim. Acta*, 260 (1995) 1.
- 7 M. Reading, A. Luget and R. Wilson, *Thermochim. Acta*, 238 (1994) 295.
- 8 A. J. Kovacs and J. M. Hutchinson, *J. Polym. Sci., Polym. Phys. Ed.*, 14 (1976) 1575.
- 9 J. M. Hutchinson and S. Montserrat, *Thermochim. Acta*, submitted.
- 10 O. S. Narayanaswamy, *J. Am. Ceram. Soc.*, 54 (1971) 491.
- 11 A. J. Kovacs, J. J. Aklonis, J. M. Hutchinson and A. R. Ramos, *J. Polym. Sci., Polym. Phys. Ed.*, 17 (1979) 1097.